



Studies of the cosmic ray energy spectrum and chemical composition at 10^{16} - 10^{18} eV with the KASCADE-Grande experiment

The KASCADE-Grande Collaboration¹

¹ Check the authors' list at the end of the article

Abstract. The KASCADE-Grande experiment operates at Karlsruhe Institute of Technology (KIT) in Germany. Its aim is the study of the primary cosmic radiation, through Extensive Air Shower detection, in the range 10^{16} - 10^{18} eV. In this contribution, KASCADE-Grande recent results will be shown, especially drawing the attention on the measurement of the cosmic ray energy spectrum.

Key words. experiment: KASCADE-Grande – cosmic ray: “knee” – cosmic ray: galactic-to-extragalactic transition – cosmic ray: all-particle spectrum – sensitivity: chemical composition

1. Introduction

The KASCADE-Grande experiment is devoted to the study of the cosmic ray primary energy spectrum and chemical composition in the range 10^{16} - 10^{18} eV. Measurements are performed indirectly, through the sampling of the Extensive Air Showers (EAS) generated by cosmic particles interacting with the atmosphere, along with the high quality reconstruction and analysis of the EAS observables. The considered primary energy range is crucial for a fulfillment of the knowledge of the cosmic ray peculiarities, because it includes both the upper part of the “knee” region of the cosmic ray energy spectrum, as well as the range in which the transition from galactic to extragalactic particles is supposed to occur.

Send offprint requests to: E. Cantoni.
e-mail: cantoni@to.infn.it

1.1. The “knee” region

The main feature of the cosmic ray all-particle energy spectrum is the so called “knee”, a break at $\sim 3 \cdot 10^{15}$ eV from a spectral index γ of ~ 2.7 to ~ 3.1 . A number of former experiments (see for example (2000) and (2000)) pointed out that the break is caused by the steepening of the light primary spectra (H, He). This finds a possible explanation in the field of the standard model (SM) for galactic cosmic rays (2000) that foresees that supernova (SN) explosions could be the sources of the particles, while supernova remnants (SNRs) could be their acceleration sites. As a consequence of magnetic confinement at acceleration and during propagation, the maximum energy the different primaries can reach (i.e. the energy at which the steepening is observed) should show a rigidity dependence $E_{max} = Z \cdot E_0 \sim Z \cdot 3 \cdot 10^{15}$ eV, being the “knee” energy E_0 roughly in agreement with the value at which SNRs get

inefficient in accelerating the particles. In this view, the “knee” of the iron component, still not detected, is expected at $\sim 10^{17}$ eV.

1.2. The galactic-to-extragalactic transition

At higher energies ($E_0 \gtrsim 10^{18}$ eV) the observed cosmic rays are expected to be of extragalactic origin basically because, there, the galactic cosmic rays gyroradius should reach the dimension of the galactic radius, so they should escape from the Galaxy. Then, in the energy range of KASCADE-Grande, several models try to explain the peculiarities of the cosmic ray energy spectrum connecting them to possible astrophysical scenarios including a transition to extragalactic sources.

In the “dip” model (2000) the break of the galactic component is foreseen at $\sim 10^{17}$ eV, the sign of transition being a so called “second knee” (observed for example by (2000) and (2000)) at about $5 - 7 \cdot 10^{17}$ eV. Then, a purely protonic extragalactic component should arise, from active galactic nuclei (AGNs). The sign of this component should be the so called “ankle”, a flattening around $3 \cdot 10^{18}$ eV (experimentally evident for example in (2000)).

In the “mixed composition model”, developed as an extension of the SM (see for example (2000) and (2000)) an extra contribution “B” of galactic cosmic rays is foreseen up to $E_0 > 10^{18}$ eV. Then the rise of an extragalactic component should occur just at the highest energies, from early active sources. The sign of the “B” component should then be the “second knee”, while the “ankle” should be the effect of the transition to the extragalactic flux.

Only deep investigations of the chemical composition in the considered energy range, though the study of the EAS observables related to primary mass, can clarify the role of the different components and to find out which is the model that better describes what is happening.

2. KASCADE-Grande main features and performances

The KASCADE-Grande experiment is a ground-based, multicomponent, air shower array. The two main components are the former KASCADE array (2000), that has been active since 1996, and the Grande array, that was realized in 2003 reassembling the detectors of the former EAS-TOP experiment (2000). The two arrays reconstruct the EAS events in cooperation (as well as independently). This is the key feature that permits to reach a high quality for the measured data (see especially (2000)).

2.1. The KASCADE array

KASCADE is sensitive to an energy range between $\sim 10^{14} - 10^{16}$, partially overlapping the Grande energy range. It is composed of 252 detector stations in a square grid of 200×200 m². In each station, the electromagnetic component and the muon component are measured separately, with two co-located but independent scintillation detectors. The unit of an electromagnetic detector is constituted by a liquid scintillator contained in a conical stainless steel box that guides the light emitted by the scintillator at the passage of the EAS particles to a photomultiplier (PMT) on top. The muon detector, constituted of a plastic scintillator, is placed below the e.m. detector, separated by a layer of iron and lead that absorbs the e.m. particles and the muons under a threshold of 230 MeV. In this case, the light emitted by the scintillator is guided by wavelength shifter bars to 4 lateral PMTs.

2.2. The Grande array

Grande extends the energy range of observations up to 10^{18} eV. This array was obtained rearranging on an area of 700×700 m² the 37 detector stations of the former EAS-TOP experiment. In the 10 m² of each station, the e.m. and muon components are measured together, as the total charged size, using a grid of 16 plastic scintillators. The Grande stations are organized in 18 exagonal clusters. At the pas-

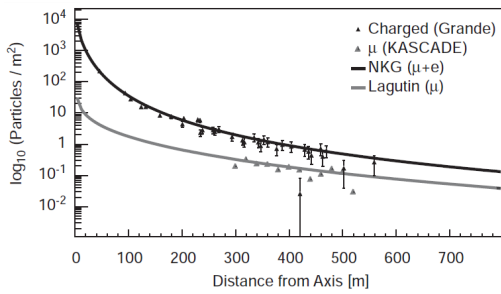


Fig. 1. A typical KASCADE-Grande well reconstructed event with its lateral distribution function. For this event the observables are: $\text{Log}_{10}(N_{ch}) = 7.0$; $\text{Log}_{10}(N_{\mu}) = 5.7$; $\theta = 24.2^{\circ}$; $\phi = 28.4^{\circ}$; $X_c = -155$ m; $Y_c = -401$ m.

sage of an EAS event, a 7-out-of-7 coincidence of a cluster triggers the data acquisition.

3. Event reconstruction, accuracies and selection

The EAS events are reconstructed in their observables with the co-operation of the two arrays. The arrival direction¹ is derived from the time differences of EAS arrival times on Grande stations, fitted with an expected distribution of the shower front through a minimum χ^2 procedure. Core position (X_c, Y_c) and total number of charged particles N_{ch} are also obtained from Grande measurements, exploiting the EAS energy deposit in each station: the evaluation of the EAS parameters is optimized through an iterative fit procedure in which the expected EAS lateral distribution function (*ldf*) is expressed as a modified Nishimura-Kamata-Greisen (NKG) formula (2000). The muon size N_{μ} is reconstructed from KASCADE measurements and the *ldf* is fitted with a Lagutin function (2000) (see figure 1).

Grande accuracies are tested through a direct comparison with KASCADE, taken as reference being a more dense experiment. A set of well reconstructed events in an area common to the two arrays is chosen and the data, independently reconstructed by the two arrays, are

¹ The zenith and azimuth angles (θ, ϕ) of the shower axis.

compared (see (2000)). A very satisfying accuracy is found for all the EAS observables: for the arrival direction $\sim 0.8^{\circ}$, for the core position ~ 6 m. The all-charged size N_{ch} is reconstructed with a systematic uncertainty $< 8\%$ and a statistical uncertainty $< 15\%$ at full efficiency (i.e. $N_{ch} > 10^6$). The accuracy for the muon reconstruction is tested with Monte Carlo simulations based on the hadronic interaction model QGSjetII (2000) with FLUKA 2002.4 for the low energy interactions (2000)². The total systematic uncertainty is kept under 10% at all muon sizes.

The final event selection takes into account runs with the detectors in stable performance and fully operational. The events must therefore pass successfully the whole KASCADE-Grande reconstruction procedure. An angular range from 0° to 40° is then chosen to avoid the bigger reconstruction uncertainties of larger angles. A fiducial area as in figure 2 is considered to discard border effects as well as under or over-estimation of N_{μ} due to the too large or too little distance from KASCADE. In this way, the total acceptance is $2 \cdot 10^9$ $\text{cm}^2 \cdot \text{sr}$. Events at full reconstruction efficiency are therefore taken (i.e. $E_0 > 10^{16}$, from simulations) so, finally, 1173 days of data taking are selected for the analysis.

4. The reconstruction of the primary energy spectrum

The cosmic ray primary energy spectrum is reconstructed taking into account the two EAS observables N_{ch} and N_{μ} provided, as shown, with high quality by KASCADE-Grande. Different methods are used, making possible the cross check of the procedures for a better evaluation of systematics and a test of the effectiveness of the hadronic interaction model used when exploiting simulations.

The first two methods can be described in parallel. They exploit the all-charged size N_{ch} or the muon size N_{μ} respectively. The Constant Intensity Cut method (CIC) is used to correct the size spectra for atmospheric attenuation

² Also further on, if not differently specified, these are the models used in simulations.

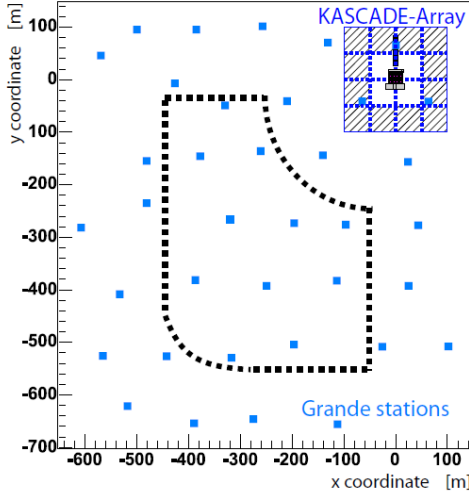


Fig. 2. The KASCADE-Grande deployment with, in dashed lines, the perimeter of the fiducial area used for the events selection.

effects. The corrected size is then calibrated with primary energy exploiting simulations. ((2000) and (2000))

To correct the resulting flux for the presence of fluctuations bigger than the bin width, an unfolding procedure is then applied. Using simulations, a “response matrix” is constructed where $R_{i,j}$ is the probability that an event reconstructed in the bin $\text{Log}[E_{rec}(i)]$ has a true energy in the bin $\text{Log}[E_{true}(j)]$. Then, the true number of events is $n_j^{true} = \sum_1^N R_{i,j} n_i^{exp}$ with N total number of bins.

The parameters obtained for the calibration formula change according to the primary element used. For this reason, also the correspondent flux will depend from the primary assumed in simulations, so that finally, a “spread” of possible fluxes is established between a pure proton and a pure iron composition (see figure 3).

4.1. The $N_{ch} - N_{\mu}$ technique

The following method aims now to give the final measurement of the primary energy spectrum (2000). In this case, using simu-

lations, a formula is derived to estimate the primary energy event by event, using both the observables N_{ch} and N_{μ} . At first, the following two expressions are calibrated for proton and iron:

$$\text{Log}(E_{H,Fe}) = a_{H,Fe} \cdot \text{Log}(N_{ch}) + b_{H,Fe} \quad (1);$$

$$\text{Log}(N_{ch}/N_{\mu}) = c_{H,Fe} \cdot \text{Log}(N_{ch}) + d_{H,Fe} \quad (2).$$

Therefore, the two expressions are put together so that:

$$\text{Log}(E_0) = (a_H + (a_{Fe} - a_H) \cdot k) \cdot \text{Log}(N_{ch}) + (b_H + (b_{Fe} - b_H) \cdot k) \quad (3)$$

with:

$$k = \frac{[\text{Log}(N_{ch}/N_{\mu}) - \text{Log}(N_{ch}/N_{\mu})_H]}{[\text{Log}(N_{ch}/N_{\mu})_{Fe} - \text{Log}(N_{ch}/N_{\mu})_H]}.$$

The k parameter is constructed in such a way that, for each event, if $k \rightarrow 0$, expression (3) tends to calibration (1) for the proton case; if $k \rightarrow 1$, (3) tends to (1) for the iron case. In this way, expression (3) takes into account the mass sensitivity, minimizing the disadvantage of depending from a certain simulated chemical composition.

The energy reconstruction is performed with (3) in 5 different angular intervals³ independently, and the results are combined afterwards (then normalizing the resulting spectrum over the whole angular range). This allows to correct for the differences in the calibration parameters due to atmospheric attenuation, as well as to take into account the shifts in the results between different angular ranges due to possible discrepancies in the air shower attenuation between real and simulated data. These differences are the first source of systematic uncertainty ($\sim 10\%$). Other sources of systematics are investigated with simulations and include: the capability to reconstruct a simulated flux (systematic $< 10\%$), the capability to assign an energy as near as possible to the true one (energy resolution $\sim 20\%$), the used simulated interaction model⁴. The cross-check with the previous techniques shows consistency by the fact that the resulting flux lies in a common range (figure 3). This

³ Of equal acceptance, between 0° and 40° .

⁴ Trials with EPOS 1.99 (2000) show it can change the intensity estimation ($-10 - 15\%$) but not the spectral structures that can appear at different energies.

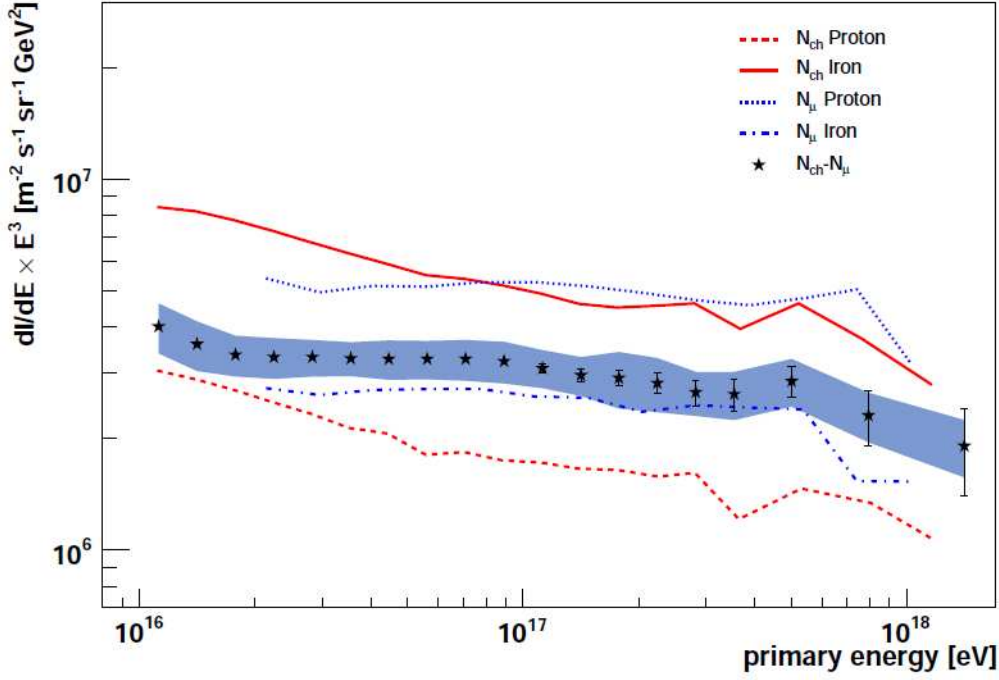


Fig. 3. The KASCADE-Grande all-particle energy spectrum reconstructed with the three different methods here illustrated. For the N_{ch} - N_{μ} technique, points are reported with the statistical error bars and the blue band representing the systematic uncertainty. For the CIC method with N_{ch} or N_{μ} , the limits deriving from H or Fe assumption in simulations are plotted in lines.

is also a confirmation of the effectiveness of the hadronic interaction model used in the exploited simulations that can describe fairly well the data even with complementary techniques.

5. Outlook on chemical composition studies

In figure 3 the resulting primary energy spectrum is shown. It presents structures under the overall power law behaviour: just over 10^{16} eV it shows a concavity, at $\sim 10^{17}$ eV it presents a small break. Chemical composition studies will be then crucial to understand the origin of this structures. Again different approaches are under study to be then cross-checked, all based on the N_{ch} and N_{μ} observables and QGSjetII model. Preliminary investigations of KASCADE-Grande sensitivity to

primary composition, based on the study of the N_{μ}/N_{ch} ratios in bins of N_{ch} to find the relative abundances of different primaries in the data (2000), show that three mass groups (light, medium and heavy) are needed to fit the experimental distributions at different energies and angles, suggesting the presence of a mixed composition, with the three components needed all over the KASCADE-Grande energy range.

6. Conclusions

KASCADE-Grande main observables, all-charged shower size N_{ch} and muon size N_{μ} are reconstructed with high precision and low systematic uncertainties. Different methods are applied and cross-checked for the reconstruction of the all-particle energy spectrum, that could be measured in the range 10^{16}

- 10^{18} eV within a 10 - 15% uncertainty, being based on the hadronic interaction model QGSjetII, which shows its intrinsic consistency. The spectrum shows structures at the threshold and around 10^{17} eV that are being investigated through chemical composition studies. The measured flux is in agreement with KASCADE and EASTOP measurements at the threshold and with HiRes and Auger measurements at the highest energies.

7. The KASCADE-Grande Collaboration

E. Cantoni^{3,7}, W.D. Apel¹, J.C. Arteaga-Velázquez², K. Bekk¹, M. Bertaina³, J. Blümer^{1,4}, H. Bozdog¹, I.M. Brancus⁵, P. Buchholz⁶, A. Chiavassa³, F. Cossavella^{4,13}, K. Daumiller¹, V. de Souza⁸, F. Di Pierro³, P. Doll¹, R. Engel¹, J. Engler¹, M. Finger⁴, D. Fuhrmann⁹, P.L. Ghia⁷, H.J. Gils¹, R. Glasstetter⁹, C. Grupen⁶, A. Haungs¹, D. Heck¹, J.R. Hörandel¹⁰, D. Huber⁴, T. Huege¹, P.G. Isar^{1,14}, K.-H. Kampert⁹, D. Kang⁴, H.O. Klages¹, K. Link⁴, P. Łuczak¹¹, M. Ludwig⁴, H.J. Mathes¹, H.J. Mayer¹, M. Melissas⁴, J. Milke¹, B. Mitrica⁵, C. Morello⁷, G. Navarra^{3,15}, J. Oehlschläger¹, S. Ostapchenko^{1,16}, S. Over⁶, N. Palmieri⁴, M. Petcu⁵, T. Pierog¹, H. Rebel¹, M. Roth¹, H. Schieler¹, F.G. Schröder¹, O. Sima¹², G. Toma⁵, G.C. Trinchero⁷, H. Ulrich¹, A. Weindl¹, J. Wochele¹, M. Wommer¹, J. Zabierowski¹¹ ⁵

¹ Institut für Kernphysik, KIT - Karlsruher Institut für Technologie, Germany; ² Universidad Michoacana, Instituto de Física y Matemáticas, Morelia, Mexico; ³ Dipartimento di Fisica Generale dell' Università Torino, Italy; ⁴ Institut für Experimentelle Kernphysik, KIT - Karlsruher Institut für Technologie, Germany; ⁵ National Institute of Physics and Nuclear Engineering, Bucharest, Romania; ⁶ Fachbereich Physik, Universität Siegen, Germany; ⁷ Istituto di Fisica dello Spazio Interplanetario, INAF Torino, Italy; ⁸ Universidade São Paulo, Instituto de Física de São Carlos, Brasil; ⁹ Fachbereich Physik, Universität Wuppertal, Germany; ¹⁰ Dept. of Astrophysics, Radboud University Nijmegen, The Netherlands; ¹¹ Soltan Institute for Nuclear Studies, Lodz, Poland;

References

- Aglietta, M., et al. 2004, *Astrop. Phys.*, 21, 583-596
 Antoni, T., et al. 2005, *Astrop. Phys.*, 24, 1-25
 Hillas, A., M. 2005, *J. Phys. G: Nucl. Part. Phys.*, 31, R95
 Berezhinsky, V., Gazizov, A. & Grigorieva, S. 2006, *Phys. Rev. D*, 74, 043005
 Nagano, M., et al. 1984, *J. Phys. G: Nucl. Phys.*, 10, L235-L239
 Bird, D., J., et al. 1993, *Ap. J.*, 424, 491
 Abraham, J., et al. 2010, *Phys. Letters B*, 685, 239-246
 Hillas, A., M. 2005, *J. Phys. G*, 31
 Allard, D., Parizot, E., Olinto, A., V. 2007, *Astrop. Phys.*, 27, 61-75
 Antoni, T., et al. 2003, *N. I. M. A*, 513, 429
 Aglietta, M., et al. 1993, *N. I. M. in Phys. Res. A*, 336, 310
 Apel, W., D., et al. 2010, *N. I. M. in Phys. Res. A*, 620, 202-216
 Apel, W., D. et al. 2006, *Astrop. Phys.* 24, 467
 Lagutin, A., A. & Raikin, R., I. 2001, *Nucl. Phys. Proc. Suppl.*, 97, 274
 Ostapchenko, S. 2006, *Nucl. Phys. B (Proc. Suppl.)*, 151, 147-150
 Fasso, A., Ferrari, A., Sala, P., R. & Ranft, J. 2000, *Proc MC 2000*, Lisbon, Portugal
 Kang, D., et al. 2009, *Proc. 31th ICRC*, Łódź, Poland, #icrc1044
 Arteaga-Velázquez, J., C., et al. 2009, *Proc. 31th ICRC*, Łódź, Poland, #icrc0805
 Bertaina, M., et al. 2009, *Proc. 31th ICRC*, Łódź, Poland, #icrc0323
 Pierog, T. & Werner, K. 2008, *Nucl. Phys. B (Proc. Suppl.)*, 196, 102-105
 Cantoni, E., et al. 2009, *Proc. 31th ICRC*, Łódź, Poland, #icrc0524

¹² Department of Physics, University of Bucharest, Bucharest, Romania;

¹³ now at: Max-Planck-Institut Physik, München, Germany; ¹⁴ now at: Institute Space Sciences, Bucharest, Romania; ¹⁵ deceased; ¹⁶ now at: Univ Trondheim, Norway.